PROCEEDINGS B

royalsocietypublishing.org/journal/rspb

Research

Cite this article: MacLaren JA. 2021 Biogeography a key influence on distal forelimb variation in horses through the Cenozoic. *Proc. R. Soc. B* **288**: 20202465. https://doi.org/10.1098/rspb.2020.2465

Received: 4 October 2020
Accepted: 11 December 2020

Subject Category:
Palaeobiology

Subject Areas:
evolution, palaeontology, ecology

Keywords:
Equidae, geometric morphometrics, locomotion, metacarpal, ordinary Procrustes analyses

Author for correspondence:
Jamie A. MacLaren
e-mail: j.maclaren@uliege.be

Electronic supplementary material is available online at https://doi.org/10.6084/m9.figshare.c.5253538.

THE ROYAL SOCIETY PUBLISHING

Biogeography a key influence on distal forelimb variation in horses through the Cenozoic

Jamie A. MacLaren[1,2]

[1]Evolution and Diversity Dynamics Laboratory, Department of Geology, Université de Liege, Building B18, Allée du Six Août 14, Sart-Tillman Campus, Liege 4000, Belgium
[2]Functional Morphology Laboratory, Department of Biology, Universiteit Antwerpen, Antwerpen 2610, Belgium

JAM, 0000-0003-4177-227X

Locomotion in terrestrial tetrapods is reliant on interactions between distal limb bones (e.g. metapodials and phalanges). The metapodial–phalangeal joint in horse (Equidae) limbs is highly specialized, facilitating vital functions (shock absorption; elastic recoil). While joint shape has changed throughout horse evolution, potential drivers of these modifications have not been quantitatively assessed. Here, I examine the morphology of the forelimb metacarpophalangeal (MCP) joint of horses and their extinct kin (palaeotheres) using geometric morphometrics and disparity analyses, within a phylogenetic context. I also develop a novel alignment protocol that explores the magnitude of shape change through time, correlated against body mass and diet. MCP shape was poorly correlated with mass or diet proxies, although significant temporal correlations were detected at 0–1 Myr intervals. A clear division was recovered between New and Old World hipparionin MCP morphologies. Significant changes in MCP disparity and high rates of shape divergence were observed during the Great American Biotic Interchange, with the MCP joint becoming broad and robust in two separate monodactyl lineages, possibly exhibiting novel locomotor behaviour. This large-scale study of MCP joint shape demonstrates the apparent capacity for horses to rapidly change their distal limb morphology to overcome discrete locomotor challenges in new habitats.

1. Introduction

Locomotion in terrestrial, volant and aquatic tetrapods is heavily influenced by the interactions between metapodials and phalanges [1–3]. One of the most recognizable and highly specialized metapodial–phalangeal joints in mammals is the 'fetlock' joint present in the feet of horses (Equidae) [4,5]. The transition of the equid forelimb from a tetradactyl (four-toed) condition to the modern monodactyl (one-toed) horse (*Equus* spp.) is a well-known example of morphological macroevolution [6]. The sister family to equids within Equoidea (the palaeotheres; Palaeotheriidae) also underwent digit reduction from tetradactyly to tridactyly (three-toes) during the Eocene and early Oligocene [7]. Eocene equids and palaeotheres were browsers with brachydont (low-crowned) dentition; species rarely exceeded 100 kg in body mass [8,9]. The last palaeotheres died out in the Oligocene of Eurasia, whereas equids proliferated in North America and began to evolve higher-crowned (hypsodont) cheek teeth [10,11]. Hypsodont dentition counteracted the higher percentage of grit and phytoliths in equid diets as they exploited more open (grassland) habitats [12]. Increases in hypsodonty were concurrent with increases in body size for many equid clades [10,13], with increasing reliance on the central digit for locomotion as the side digits became more reduced [6]. By contrast, palaeotheres evolved large sizes in the Eocene (e.g. [8]) prior to their near-complete disappearance at the 'Grande Coupure' [14]. Turnover events, such as regional extinctions and biogeographic dispersals, have not been examined as impactors

of equoid locomotor evolution, despite multiple such events occurring throughout the Cenozoic [15–17]. Shifts in metapodial–phalangeal joint morphology during novel habitat exploitation may demonstrate the functional plasticity of the joint in equoids. For example, prominence of the metacarpal sagittal ridge would indicate an increase in stability and reduction in adduction or abduction at the joint [18]; similarly, mediolateral expansion of the metacarpal head would dissipate compressive forces associated with body mass increases [19].

In this study, I investigate the morphology of the central forelimb metapodial joint surface, the metacarpophalangeal joint (MCP joint), across Equoidea. The forelimb was chosen as, unlike the hind limb, it undergoes full digit reduction from four functional digits to one during equid evolution [6]. Using a geometric morphometric approach to quantify MCP joint shape, I combine traditional and novel alignment protocols to assess the magnitude of divergence in each phenotype from an ancestral morphology, and examine shape changes with respect to intrinsic biological traits (mass/tooth crown height) and extrinsic environmental drivers. As digit reduction and the adoption of the spring-foot morphology in equids predate the evolution of hypsodont dentition [20], I do not anticipate a strong temporal correlation between changes in MCP joint shape and hypsodonty. However, owing to the intimate link between body mass and limb bone dimensions [21], I predict MCP joint shape changes will be correlated with temporal fluctuations in body mass. Finally, I anticipate that regional extinctions and dispersal events will be reflected in morphofunctional changes in MCP joint shape.

2. Methodology

(a) Specimen sampling and phylogeny

A total of 217 distal third metacarpals were laser surface scanned representing 55 species of extant and extinct equoids. As a broad phylogenetic analysis of all equoid relationships is presently unavailable, I constructed an informal phylogenetic supertree in Mesquite v. 3.04 from 19 published sources, incorporating all equids and palaeotheres in the study, and exported to R v. 3.6.3 [22]. The phylogeny was time calibrated using occurrence data from the Palaeobiology Database. I applied two distinct time calibration procedures (maximum and minimum ages) to account for uncertainty of node ages using 'paleotree' v. 3.3.25 [23]. Additional details related to the laser scanner specifications and phylogenetic reconstruction can be found in the electronic supplementary material.

(b) Geometric morphometrics

MCP joint morphology was quantified using 17 Type II landmarks [24] representing homologous features on the metacarpal head, applied in Landmark Editor v. 3.0 [25] (figure 1*a*; electronic supplementary material, figure S1). Configurations were subjected to two alignment procedures. Generalized Procrustes analysis (GPA) yielded overall Procrustes coordinates which were used for principal components analysis (PCA) to examine patterns of shape variation across the sample; the time-calibrated phylogeny was mapped onto the PCA to generate a phylomorphospace using 'phytools' v. 0.7-20. Secondly, raw landmark coordinates were individually aligned against a hypothetical ancestral equoid metacarpal shape using an iterative ordinary Procrustes analyses (OPA) to calculate the magnitude of shape divergence between each tip taxon and the ancestor using the *procOPA()* function in 'shapes' v. 1.2.5 [26]. This method reduces data transformation while determining which MCP joints changed shape most greatly from their ancestral morphology. Resultant species averaged divergence magnitudes (ordinary sums of square distances) were used as a proxy for MCP joint divergence from the ancestral shape. Details of ancestral shape generation and iterative OPA can be found in the electronic supplementary material. MCP joint divergence values were examined on the time-calibrated phylogeny to estimate rates of shape divergence from the ancestral morphology through time using 'geiger' v. 2.0.6.4, 'phytools' v. 0.7-20 and 'RRphylo' v. 2.4.0 [27–29]. Owing to uncertainty of branching ages, rates of trait evolution were estimated for both maximal and minimal ages of taxa; results were compared using the *ccf()* function in 'stats' v. 3.6.3 [30] to identify correlated shifts at nodes. Rate shifts were then projected onto the phylomorphospace. Node rates are provided in the electronic supplementary material, table S2.

(c) Disparity

I used the dispRity v. 1.2.3 package [31] to assess MCP joint disparity across four turnover events: the 'Grande Coupure' (33.9 Ma); Mid-Miocene Climatic Optimum (MMCO; *ca*. 18–14 Mya); the Vallesian 'Crisis' (9–11 Ma); and the formation of the Isthmus of Panama (2–4 Ma). Disparity was calculated using a sum of variances metric with a bootstrapping procedure (500 iterations) based on principal component (PC) scores for taxa either side of each turnover event, with non-parametric Wilcoxon tests for significant differences conducted in 'stats' v. 3.6.3. Results from different bootstrapping regimes (2000, 1000, 500, 250 iterations) indicated the necessity for an α-value of 0.01 (99% confidence) for disparity results to avoid false positives; see the electronic supplementary material for details.

(d) Covariates

Hypsodonty index (M2 crown height ÷ M2 crown width; [32]) and natural logarithm of body mass were used as covariates for comparison with MCP joint shape coordinates and divergence values; sources, values and calculations for covariates can be found in the electronic supplementary material. Covariates were regressed against GPA-aligned shape coordinates using a phylogenetic partial least square (PPLS) regression in MorphoJ [33] using independent contrasts to account for phylogenetic relatedness and assessed using an RV coefficient (multivariate generalization of squared Pearson correlation coefficient) [33]. Hypsodonty, body mass and MCP joint divergence magnitudes were tested for overall correlation using a Phylogenetic generalized least square (PGLS) regression for univariate data using 'caper' 1.0.1. Finally, first differences between average hypsodonty, body mass and MCP joint divergence magnitudes were calculated for successive time-bins and the time series were tested for cross-correlations using the *ccf()* function in 'stats' v. 3.6.3. Further details of correlation analyses can be found in the electronic supplementary material.

3. Results

(a) Metacarpal morphology and rates of evolution

The morphological variation in MCP joint using fixed point landmarks on the metacarpal head was visually examined using a phylomorphospace (figure 1*a*,*b*), with rates of MCP joint divergence plotted onto the phylogeny of equoids (see also electronic supplementary material, figure S2). MCP joint divergence for the maximum and minimum branch length protocols were compared using cross-correlation; patterns of trait evolution between nodes corresponded significantly

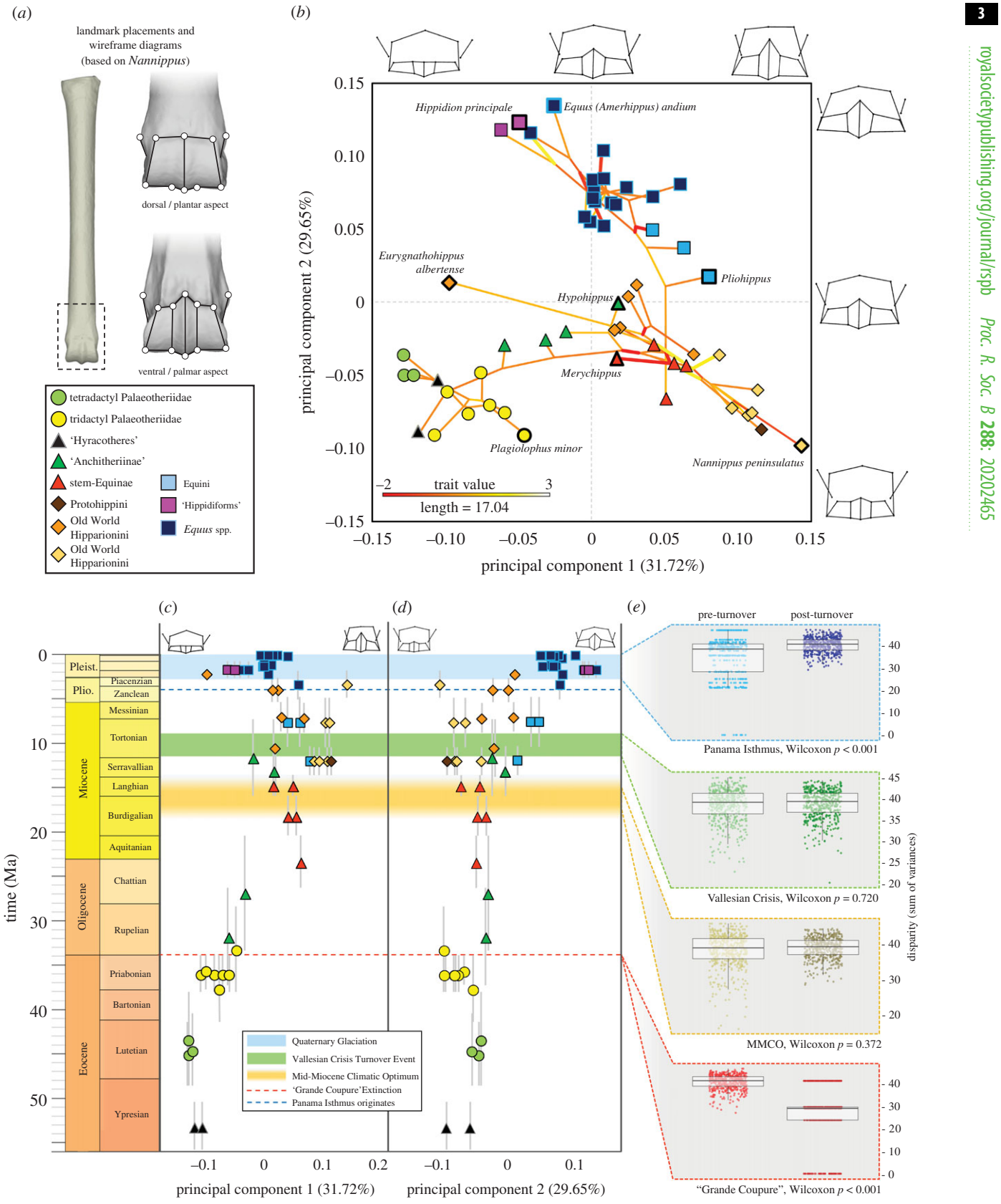

Figure 1. Patterns of equoid MCP shape. (*a*) Schematic demonstrating landmark placements on the distal metacarpal, with taxonomic key detailing symbols and colours for phylogenetic clades. (*b*) Phylomorphospace based on first two PCA axes of equoid metacarpal head morphology (accounting for 61.37% variation), with evolutionary rate of MCP joint divergence superimposed onto the phylogeny. Greatest deviations from the baseline rate of evolution are highlighted with bold lines (light, increased rate; dark, decreased rate). Key taxa labelled and highlighted with bold outlines. (*c*) Variation in equoid metacarpal head morphology along principal component 1 (31.72%) plotted through time; (*d*) variation in equoid metacarpal head morphology along principal component 2 (29.65%) plotted through time. Grey bars in (*b*) and (*c*) denote lineage duration. (*e*) Disparity (sum of variances) of MCP joint shape across four Cenozoic turnover events. (from top) Isthmus of Panama (Great American Biotic Interchange); Vallesian Crisis Turnover Event; Mid-Miocene Climatic Optimum (MMCO); 'Grande Coupure' (Eocene–Oligocene extinction event). Wilcoxon *p*-values denote the significance of change in disparity. (Online version in colour.)

and strongly ($R = 0.727$). Hereafter, rates of evolution along branch lengths will refer to those from the maximum ages tree (see the electronic supplementary material, S7, figure S2).

Basal equoid MCP joint morphologies are characterized by relatively broad metacarpal heads, sagittal ridges restricted to the palmar aspect (articulating only with the sesamoids), and prominent collateral ligament attachments (figure 1*b*; wireframes). Species exhibiting this morphology include palaeotheres and 'hyracotheres', all of which occupy regions of negative PC1 and PC2 phylomorphospace (figure 1*b*). Rates of MCP joint divergence in basal equoids are similar to the average rate for the entire tree (figure 1*b*; electronic supplementary material, table S2). The MCP joint divergence magnitude of anchitheres (*Mesohippus*, *Miohippus*, *Hypohippus*, *Anchitherium*) also exhibits evolutionary rates similar to the background rate of 0 (figure 1*a*; electronic supplementary material, figure S2). Despite no discernible shift in evolutionary rate, anchitheres demonstrate a gradient of MCP joint morphology, culminating in the derived *Equus*-sized *Hypohippus* exhibiting a flared metacarpal head with broad articulations (akin to modern equids), but retaining a low, discrete dorsal (anterior) sagittal ridge (figure 1). The first major reduction in MCP joint divergence rate is observed between anchitheres and *Archaeohippus–Parahippus* group (figure 1*b*; node 70–72; electronic supplementary material, figure S2). *Archaeohippus* and *Parahippus* exhibit mediolaterally narrow metacarpals with more prominent sagittal ridges than anchitheres (figure 1*b–d*), similar in shape to the derived New World (NW) hipparionins (figure 1*b–d*), with which these species share small body sizes (electronic supplementary material, table S3). Overall, the tribe Equini (non-hipparionin equines) exhibit limited changes from the average rate of MCP joint divergence. Equinin MCP joint shapes occupy exclusively positive PC2 morphospace (figure 1*b*,*d*), defined by a strongly prominent sagittal ridge and outwardly flared articulation surfaces (figure 1*b*,*d*; wireframes). The most notable rate changes within the Equini occur within the South American endemics *Hippidion principale* (higher rate of divergence than average) and *Equus* (*Amerhippus*) *santaeelenae* (lower rate of divergence than average for the tree). Several South American equinins developed highly robust metapodial morphologies (figure 1*b*; top left of morphospace) not present prior to the invasion of South America, exhibiting very broad metacarpal heads, prominent collateral ligament attachments and steep sagittal ridges. The opposite is true for the Hipparionini; a very sharp increase away from the average metacarpal divergence rate is observed at the base of this clade (node 97–98; electronic supplementary material, figure S2) as it splits from the stem equine *Merychippus*-morphology (figure 1*b*; electronic supplementary material, figures S2 and S9). NW hipparionins exhibit mediolaterally narrow metapodials, with strongly flared phalangeal and sesamoid joint articulations, and prominent sagittal ridges keeping the phalanges in near-parasagittal rotation. Several taxa, such as *Nannippus peninsulatus*, plot the furthest from the basal equid (hyracothere) MCP joint condition (figure 1*b–d*; electronic supplementary material, figure S9), and exhibit some of the highest MCP joint divergence magnitudes (electronic supplementary material, table S1). A rapid increase in the rate of MCP joint evolution occurs at the origin of Old World (OW) hipparionins (node 104 + 105; electronic supplementary material, figure S2). This rate shift is associated with a mediolateral expansion of the metacarpal head, resulting in OW hipparionin MCP joint morphologies similar to derived anchitheres (figure 1*b*; electronic supplementary material, table S3 and figure S9). OW hipparionins (with the exception of the highly robust *Eurygnathohippus albertense*) exhibit a narrower range of MCP joint divergence magnitudes by contrast to NW hipparionins (electronic supplementary material, table S3). Following the initial rate increase at the origin of OW hipparionins, rates of MCP joint divergence remain close to the baseline rate of evolution (figure 1*b*; electronic supplementary material, table S2, figures S2 and S9).

(b) Disparity across turnover events

Results from comparisons in MCP joint shape disparity (based on PC scores for all axes) across turnover events are displayed in figure 1*e*. Disparity significantly drops across the 'Grande Coupure' (33.9 Ma) ($p < 0.01$), reflecting the loss of almost all palaeothere species; the resultant disparity in the earliest Oligocene is low, but poorly resolved owing to low species count. Although equid taxon diversity increases through the MMCO (*ca* 18–14 Ma), analyses do not suggest well-supported significant differences in MCP joint disparity. This may be owing to low sampling of taxa following the MMCO; however, the existence of a broad range of MCP joint morphologies between anchitheriine and stem equinines lends support to a non-significant result. The Vallesian Turnover Event (11–9.7 Ma) also yielded no significant difference in MCP joint disparity. Highly significant differences in MCP joint disparity were observed ($p < 0.01$) between the onset of the Panamanian Isthmus and its completion (*ca* 4–2 Ma). The co-occurrence of highly derived South American equids drove this significant increase in MCP joint disparity; removal of South American equinins results in a significant decrease (rather than increase) in disparity (electronic supplementary material, figure S8). Significance values for all disparity comparisons are tabulated in the electronic supplementary material, table S6.

(c) Correlation analyses

PGLSs regressions of MCP joint divergence magnitudes against intrinsic biological traits revealed weak significant correlations between equoid MCP joint divergence magnitudes and hypsodonty ($R^2 = 0.126$; $p < 0.01$) and body mass ($R^2 = 0.021$; $p = 0.01$); no significant PGLS correlation was detected between hypsodonty and body mass ($R^2 = 0.000$; $p = 0.969$) (electronic supplementary material, figure S4 and table S4). PPLS regressions of Procrustes aligned shape variables against hypsodonty and body mass show weak and non-significant correlations between equoid MCP joint shapes (hypsodonty (RV = 0.077; partial least square axes regression = 0.488; correlation $p = 0.209$) or body mass (RV = 0.070; PLS correlation = 0.413; correlation $p = 0.579$; electronic supplementary material, figure S5 and table S5).

Cross-correlations comparing first differences of average MCP joint divergence magnitudes with hypsodonty and body mass through time suggest weak but significant temporal correlations between 0 Myr and 1 Myr lag time (MCP joint divergence versus hypsodonty: 0 Myr $R = 0.367$, 1 Myr $R = 0.296$; MCP joint divergence versus body mass: 1 Myr $R = 0.364$) (electronic supplementary material, figure S6). These significant correlations indicate shifts in average joint divergence and are correlated positively with concurrent

changes hypsodonty (0 Ma), and also weakly positively correlated with changes in hypsodonty and body mass which occurred *ca* 1 Ma later (electronic supplementary material, figure S6). Fluctuations in body mass and hypsodonty index are recovered as strongly and significantly temporally correlated (0 Ma $R = 0.939$) (electronic supplementary material, figure S6).

4. Discussion

This study set out to quantify the evolution of the MCP joint of equoids across a broad temporal and geographical scope, to investigate its relationship to size and diet proxies, and examine whether turnovers or geographical dispersals correlated with significant changes in shape or rate of shape evolution. Results support weak but significant temporal correlations between changes in hypsodonty (diet proxy) and body mass with changes in the locomotor morphology of equoids; however, overall correlations between these traits are comparatively weak. This study also highlights discrete rate shifts in MCP joint evolution, with some changes in MCP joint disparity occurring in conjunction with environmental drivers, namely extinction events and biogeographic dispersals.

(a) Correlation of shape, size and ecology

Correlating morphological traits of biological organisms should be carried out while maintaining the understanding that those traits all comprise the animal as a whole, rather than necessarily standing alone as features uninfluenced by other aspects of the biology of the organism [34]. With this understanding there comes an expectation that certain aspects of an animal's biology will change together, or will be somewhat correlated (i.e. integrated traits). Within the present study, correlation analyses indicated weak correlations between hypsodonty and MCP joint shape (electronic supplementary material, figures S3–S5 and tables S3–S5), with exceptionally weak coefficients when incorporating phylogeny (electronic supplementary material, tables S4 and S5). Surprisingly, shifts in MCP joint shape and tooth crown height (hypsodonty) were shown to be significantly correlated using cross-correlation of first differences, within a temporal range of 0–1 Myr (electronic supplementary material, figure S6). In other words, a significant positive correlation exists between changes in hypsodonty occurring concurrently ($R = 0.367$) or 1 Myr later ($R = 0.296$) than changes in MCP joint shape (electronic supplementary material, figure S6). These positive correlations were significant, but not strong. Although phylogenetic relatedness could not be accounted for in cross-correlation analyses, results from overall phylogenetic regressions suggested a decrease in both regression coefficients and statistical significance with the inclusion of phylogenetic information (electronic supplementary material, figures S4 and S5 and tables S4 and S5). Fluctuations in the average MCP joint divergence magnitude correlated predominantly with fluctuations in hypsodonty throughout the late Cenozoic (electronic supplementary material, figure S7), suggesting the potential for higher integration between changes in feeding and locomotor morphology within species from the Miocene to Holocene than pre-Miocene. Despite NW and OW hipparionin MCP joint shape differing (figure 1*b*), successive replacement of earlier species by later ones in both lineages probably lead to the consistent MCP joint disparity signal observed (figure 1*c*,*d*); this contrasts with overall hypsodonty and body mass patterns within equids (e.g. [10,32]). Correlations of body mass with MCP joint morphology indicate a similar pattern, with overall correlations suggesting weak, and in some cases non-significant, relationships (electronic supplementary material, figures S3–S5 and tables S3–S5). Again, cross-correlations suggest weak but significant positive temporal correlation between average changes in body mass and average MCP joint divergence magnitude ($R = 0.364$) in the sample. Notable temporal correlations between average body mass and MCP joint divergence occur at the origins of *Palaeotherium* genus (38 Ma) and the origin of the subfamily Equinae (13.6 Ma) (electronic supplementary material, figure S7).

As recent authors have hypothesized (e.g. [35–37]), the interplay between intrinsic biological traits (in addition to body mass) and extrinsic ecological factors is most likely associated with selection pressures at local or species-level scales, with multiple micro-evolutionary changes leading to the patterns of morphological expression observed in the equid locomotor and feeding apparatuses. This study demonstrates that derived and highly hypsodont NW hipparionins (such as *Nannippus*) drive MCP joint morphological variation into new regions of morphospace (figure 1*b*; positive PC1 region), quite separate from ancestral basal equids (figure 1), and also separate from derived equinins and OW hipparionins (figure 1*b*). Small body masses (ranging from approximately 50–150 kg; see also [32]) coupled with quite unique MCP joint morphology and high-crowned teeth represent a local-level suite of biological traits exhibited by NW hipparionins. The youngest of these genera (*Nannippus*) were in potential competition with the increasingly large and monodactyl equinins (e.g. *Astrohippus* and *Dinohippus*). Competition avoidance may, therefore, have driven *Nannippus* to retain very small body sizes (approximately 50–75 kg) so as not to compete directly with large equinins in a shared feeding niche [37]. Consequently, their distal limbs would not be selected for high loading owing to increased body masses, leading to gracile MCP joint morphologies (figure 1*b*). This study suggests that temporal correlations between shifts in locomotor morphology, body mass and dietary proxies are tenuously linked, with correlations in small numbers of species displaying a combination of traits driving the divergence of the organism as a whole (figure 1; electronic supplementary material, figures S7 and S8). Results compliment other large-scale investigations into equid ecology and macroevolution [10,32]. Staggered increases in dental mesowear [10], body mass, hypsodonty [10,32] and MCP joint divergence through the Miocene and Pliocene are suggestive of localized or species-specific changes affecting the overall increase in these trait values (electronic supplementary material, figure S7, also see [10]). By contrast, diversification pulses have not been shown to closely correlate with phenotypic evolution in equids [32]; my results corroborate these findings, with no significant increase in MCP joint disparity during the Miocene (figure 1*e*) despite it being regarded as an epoch of accelerated equid diversification (e.g. [38]). Diversity dynamics in equids have also previously been linked to geographical dispersals [32], which offer release from ecomorphological constraints. Biogeographic and turnover signals were recovered in this morphological study, with two events exhibiting significant impact on equoid locomotor morphology: the 'Grande

Coupure' (Eocene–Oligocene extinction event), and the migration of equinins into South America.

(b) Extinction, migration and morphological disparity

The Cenozoic has played host to many faunal turnover events (e.g. [39,40]). The four events investigated in this study were anticipated to demonstrate shifts in MCP joint morphology and rates of morphological change owing to their established impact on equoid community structure. Biological changes (e.g. morphology) on any temporal or spatial scale as a response to migration or localized extinction are difficult to pinpoint [41]; however, the loss of phenotypic diversity following extinction events is a well-known phenomenon. The 'Grande Coupure' extinction event is clearly reflected in the results of this study with a highly significant decrease in MCP joint disparity ($p < 0.01$) across the Eocene–Oligocene boundary (figure 1*c–e*; electronic supplementary material, figure S7 and table S6). The 'Grande Coupure' is well recognized in Europe [40], but has yet to be associated with widespread community changes in North America [42]. The results of the present study indicate that global equoid locomotor diversity across the Eocene–Oligocene boundary was dramatically reduced with the loss of multiple palaeothere taxa (figure 1*c–e*). The diversity of form in palaeothere locomotor anatomy has recently been quantitatively examined [8]. Equoid disparity prior to the 'Grande Coupure' supports these previous findings, and the loss of phenotypic diversity following the extinction of the morphologically diverse genus *Palaeotherium* (figure 1*c–e*) is, therefore, an unsurprising result from this study. Morphological examination of *Plagiolophus minor* (of one of the few palaeotheres to persist beyond the 'Grande Coupure') has highlighted potential locomotor advantages for small, cursorial ungulates in the drier, cooler habitats of post-Eocene Europe [8,43]. The placement of plagiolophine MCP joints in morphospace suggests that the sagittal keel of these species was less prominent than in contemporaneous true equids at this early stage of their evolution (figure 1*b*; electronic supplementary material, figure S8). The development of the sagittal keel through equid evolution has been associated with increasing MCP joint range of motion [4] and stability in straight line running [18]. Such a subtle difference in the MCP joint is unlikely to have played a strong role in the ultimate extinction of palaeotheres, and given a lack of experimental evidence, this study will not ascribe any specific adaptive advantage to the equid MCP joint over that of palaeotheres in the aftermath of the 'Grande Coupure'. Although these taxa have been known to science for hundreds of years, further comparative studies of Eocene equid and palaeothere locomotor morphology will be required to decipher any locomotor advantage in the equid distal limb apparatus above that of palaeotheres. However, locomotor advantage may play a key role in explaining the increase in disparity following the formation of the Panamanian Isthmus (figure 1*e*) and subsequent migration of equids into South America.

The formation of the Isthmus of Panama offered a landbridge for North American equids to disperse into South America in the late Pliocene [44]. Two genera of equinins (*Equus* (*Amerhippus*) and *Hippidion*) are known to have made this transition prior to 2.5 Ma, and both genera include species with highly robust metapodia [45]. The extremely broad MCP joints of *Hippidion* spp., *E.* (*Amerhippus*) *andium* and *E.* (*A.*) *neogeus* place them as some of the most divergent MCP joints in this study (figure 1*b–d*; electronic supplementary material, table S1). Following the Panamanian Isthmus completion, MCP joint disparity and average MCP joint divergence magnitude decline (figure 1*e*; electronic supplementary material, figure S7). Disparity increase is driven by the presence of robust South American species (electronic supplementary material, figure S8), which explore new regions of metacarpal morphospace (negative PC1/positive PC2; figure 1*c,d*). The metacarpal head of South American equinins is broader than other equinin species (figure 1*b*), a morphology present in both large (approximately 520 kg) and small (approximately 220 kg) taxa [46], and species with high and mid-range hypsodonty values (e.g. *E.* (*A.*) *neogeus* = 4.0; *Hi. devillei* = 2.4) [32]. Biogeographic evidence supports an initial migration of both genera south along the Andes [44]; the closest phylogenetic relatives to the extremely robust *E.* (*A.*) *andium* and *E.* (*A.*) *neogeus* do not exhibit highly robust metacarpal morphologies (e.g. *E.* (*A.*) *insulatus*; electronic supplementary material, figure S5). Fossils of the most robust taxa (*Hippidion* and *E.* (*A.*) *andium*) have been found at altitudes between 2000 and 3900 m, whereas the younger and less robust *E.* (*A.*) *insulatus* and *E.* (*A.*) *santaeelenae* are known from lower altitudes (100–2500 m; altitudes from Paleobiology Database). High-altitude habitat occupation by robust equinins may represent evidence of a perissodactyl form of a 'low-gear' locomotor morphology [47]. Low-gear locomotion is a method of low-speed walking in mountainous terrain exhibited by a wide range of artiodactyls, often associated with short and broad distal limb bones [48]. This phenomenon is known within insular populations evolving in predator-free environments [47], and is also exhibited in bovine artiodactyls inhabiting mountainous regions with low topographical complexity [48]. The robust South American equinin metapodials with broad articular surface to dissipate loading forces, large areas for collateral, and suspensory ligament attachment [49] would have conferred a high degree of stability for the distal monodactyl forelimb [50], ideal for negotiating unstable or inclined substrates [48]. These convergent morphologies between two monodactyl lineages suggest that equinins migrating to South America underwent similar selective pressures to their locomotor apparatus, potentially resulting in a 'low-gear' locomotor mode akin to mountain-dwelling artiodactyls [48]. Evolutionary rates evidence suggests that MCP joint divergence in *Hi. principale* was much faster than the base rate (figure 1*b*; electronic supplementary material, figure S2), and the same is true for the clade enclosing *E.* (*A.*) *andium* and *E.* (*A.*) *neogeus* (compared to their closest relative *E.* (*A.*) *santaeelenae*) (figure 1; electronic supplementary material, figures S2 and S9). Although experimental evidence will be required before a more definitive conclusion can be made, the results from this study lead me to hypothesize that the robust metapodials of South American equinins were the result of a rapid convergent response to a localized selection pressure in the form of a more steeply inclined, higher altitude habitat than monodactyl equids had previously encountered [44]. Evidence from generations of selective breeding of domestic horses (*E. caballus*) demonstrate the capacity for equids to exhibit highly variable limb morphologies under artificial selection (e.g. [51]). The morphological response to local environment in robust South American equinins also occurred over a short geological time, with high evolutionary rates

particularly in the hippidiform lineage (figure 1*b*; electronic supplementary material, figure S2). These results demonstrate the apparent ability for monodactyl equids to rapidly modify their distal locomotor apparatus in response to localized habit demands.

5. Conclusion

The MCP joint is a pivotal anatomical unit for understanding the locomotor evolution of equoids. In this study, I developed a novel, iterative alignment procedure to quantify divergence from ancestral morphology, and related changes in the distal metacarpal across a broad spatiotemporal sample of equoids. Contrary to initial expectations, both body mass and hypsodonty showed limited correlation with MCP joint shape; however, significant temporal correlations between all three traits were identified. A significant decrease in MCP joint disparity was recovered at the Eocene–Oligocene extinction event with the loss of many morphologically diverse palaeotheres; however, MCP joint disparity through Miocene turnover events was revealed to be stable, perhaps indicating consistent locomotor demands during the radiation of equids during the middle Miocene. Most notably, the dispersal of equinins into South America yielded a dramatic increase in MCP joint disparity and divergence magnitude. The invasion of virgin territory by derived equids drove morphological variation in the MCP joint, promoting forelimb stability, locomotor efficiency and force dissipation. In a broader sense, this study demonstrates the apparent ability for monodactyl horses to rapidly adapt their locomotor anatomy to meet the demands of their habitat, highlighting their adaptability in response to localized selective pressures.

Data accessibility. Electronic supplementary material linked to the article can be found from the Dryad Digital Repository: https://doi.org/10.5061/dryad.x0k6djhhg [52]. Electronic supplementary material includes: Supplementary Methodology and Figures, list of Specimens, Landmark Coordinate files, Covariates and Correlation analyses, Phylogenetic Supertree, R codes, MorphoJ project file, and three-dimensional models. Three-dimensional models used in this study will also be accessible via Morphosource.org (project: 'MacLaren (2021) Equoid metacarpal 3D models') following agreement from institutions.

Competing interests. I declare I have no competing interests.

Funding. This study was funded by Fonds Wetenschappelijk Onderzoek (FWO) and Fonds de la Recherche Scientifique (FRS–FNRS), and travel grants from the FLMNH and EAVP.

Acknowledgements. I wish to thank the museum staff at the MuseOs, MuMo, RMCA (Belgium); AMNH, FLMNH, MCZ, MVZ, OMNH (USA); MNHN, UCBL (France); GMH, MfNB (Germany); NHMW (Austria); NHMUK (UK); Naturalis (The Netherlands). I extend thanks to S. Nauwelaerts, P. Aerts, my doctoral committee members, V. Fischer, C. Janis and an anonymous reviewer for manuscript suggestions.

References

1. Bonnan MF. 2003 The evolution of manus shape in sauropod dinosaurs: implications for functional morphology, forelimb orientation, and phylogeny. *J. Vertebr. Paleontol.* **23**, 595–613. (doi:10.1671/A1108)
2. Nyakatura JA. 2012 The convergent evolution of suspensory posture and locomotion in tree sloths. *J. Mamm. Evol.* **19**, 225–234. (doi:10.1007/s10914-011-9174-x)
3. Druelle F, Young J, Berillon G. 2018 Behavioral implications of ontogenetic changes in intrinsic hand and foot proportions in olive baboons (*Papio anubis*). *Am. J. Phys. Anthropol.* **165**, 65–76. (doi:10.1002/ajpa.23331)
4. MacFadden BJ. 1992 What's the use? Functional morphology of feeding and locomotion. In *Fossil horses: systematics, paleobiology, and evolution of the family equidae*, pp. 229–262. Cambridge, UK: Cambridge University Press.
5. Thomason JJ. 1986 The functional morphology of the manus in the tridactyl equids *Merychippus* and *Mesohippus*: paleontological inferences from neontological models. *J. Vertebr. Paleontol.* **6**, 143–161. (doi:10.1080/02724634.1986.10011607)
6. McHorse BK, Biewener AA, Pierce SE. 2019 The evolution of a single toe in horses: causes, consequences, and the way forward. *Integr. Comp. Biol.* **59**, 638–655. (doi:10.1093/icb/icz050)
7. Bai B. 2017 Eocene Pachynolophinae (Perissodactyla, Palaeotheriidae) from China, and their palaeobiogeographical implications. *Palaeontology* **60**, 837–852. (doi:10.1111/pala.12319)
8. MacLaren JA, Nauwelaerts S. 2020 Modern tapirs as morphofunctional analogues for locomotion in endemic Eocene European perissodactyls. *J. Mamm. Evol.* **27**, 245–263. (doi:10.1007/s10914-019-09460-1)
9. Ring SJ, Bocherens H, Wings O, Rabi M. 2020 Divergent mammalian body size in a stable Eocene greenhouse climate. *Sci. Rep.* **10**, 1–10. (doi:10.1038/s41598-020-60379-7)
10. Mihlbachler MC, Rivals F, Solounias N, Semprebon GM. 2011 Dietary change and evolution of horses in North America. *Science* (*80-.*) **331**, 1178–1181. (doi:10.1126/science.1196166)
11. Levering D, Hopkins S, Davis E. 2017 Increasing locomotor efficiency among North American ungulates across the Oligocene-Miocene boundary. *Palaeogeogr. Palaeoclimatol. Palaeoecol.* **466**, 279–286. (doi:10.1016/J.PALAEO.2016.11.036)
12. Semprebon GM, Rivals F, Janis CM. 2019 The role of grass vs. exogenous abrasives in the paleodietary patterns of North American ungulates. *Front. Ecol. Evol.* **7**, 65. (doi:10.3389/fevo.2019.00065)
13. MacFadden BJ. 1986 Fossil horses from '*Eohippus*' (*Hyracotherium*) to *Equus*; scaling, Cope's law, and the evolution of body size. *Paleobiology* **12**, 355–369. (doi:10.1017/s0094837300003109)
14. Joomun SC, Hooker JJ, Collinson ME. 2008 Dental wear variation and implications for diet: an example from Eocene perissodactyls (Mammalia). *Palaeogeogr. Palaeoclimatol. Palaeoecol.* **263**, 92–106. (doi:10.1016/j.palaeo.2008.03.001)
15. O'Dea A *et al.* 2016 Formation of the isthmus of Panama. *Sci. Adv.* **2**, 1–12. (doi:10.1126/sciadv.1600883)
16. Casanovas-Vilar I, Van Den Hoek Ostende LW, Furió M, Madern PA. 2014 The range and extent of the Vallesian Crisis (Late Miocene): new prospects based on the micromammal record from the Vallès-Penedès basin (Catalonia, Spain). *J. Iber. Geol.* **40**, 29–49. (doi:10.5209/rev_JIGE.2014.v40.n1.44086)
17. Fraser D, Gorelick R, Rybczynski N. 2015 Macroevolution and climate change influence phylogenetic community assembly of North American hoofed mammals. *Biol. J. Linn. Soc.* **114**, 485–494. (doi:10.1111/bij.12457)
18. Sondaar PY. 1968 The osteology of the manus of fossil and recent Equidae. *Verh. der K. Ned. Akad. van Wet. Natuurkd.* **25**, 1–76.
19. McHorse BK, Biewener AA, Pierce SE. 2017 Mechanics of evolutionary digit reduction in fossil horses (Equidae). *Proc. R. Soc. B* **284**, 20171174. (doi:10.1098/rspb.2017.1174)
20. MacFadden BJ. 2005 Fossil horses—evidence for evolution. *Science* (*80-.*) **307**, 1728–1730. (doi:10.1126/science.1105458)
21. Scott KM. 1990 Postcranial dimensions of ungulates as predictors of body size. In *Body size in mammalian paleobiology: estimation and biological implications* (eds J Damuth, BJ MacFadden),

pp. 301–335. Cambridge, UK: Cambridge University Press.

22. RStudioTeam. 2016 RStudio: integrated development for R. See http://www.rstudio.com/.
23. Bapst DW. 2012 paleotree: an R package for paleontological and phylogenetic analyses of evolution. *Methods Ecol. Evol.* **3**, 803–807. (doi:10.1111/j.2041-210X.2012.00223.x)
24. Rohlf FJ, Slice DE. 1990 Extensions of the Procrustes method for the optimal superimposition of landmarks. *Syst. Zool.* **39**, 40–59. (doi:10.2307/2992207)
25. Wiley DF *et al.* 2006 *Landmark editor 3.0*. Davis, CA: Institute for Data Analysis and Visualization, University of California.
26. Dryden IL, Mardia KV. 2016 The shapes package in R. In *Statistical shape analysis with applications in R* (eds IL Dryden, K V. Mardia), pp. 6–7. Chichester, UK: Wiley.
27. Garland T, Dickerman AW, Janis CM, Jones JA. 1993 Phylogenetic analysis of covariance by computer simulation. *Syst. Biol.* **42**, 265–292. (doi:10.1093/sysbio/42.3.265)
28. Revell LJ. 2012 phytools: an R package for phylogenetic comparative biology (and other things). *Methods Ecol. Evol.* **3**, 217–223. (doi:10.1111/j.2041-210X.2011.00169.x)
29. Castiglione S, Tesone G, Piccolo M, Melchionna M, Mondanaro A, Serio C, Di Febbraro M, Raia P. 2018 A new method for testing evolutionary rate variation and shifts in phenotypic evolution. *Methods Ecol. Evol.* **9**, 974–983. (doi:10.1111/2041-210X.12954)
30. R Core Development Team. 2008 *R: a language and environment for statistical computing*. Vienna, Austria: R Foundation for Statistical Computing.
31. Guillerme T. 2018 dispRity: a modular R package for measuring disparity. *Methods Ecol. Evol.* **9**, 1755–1763. (doi:10.1111/2041-210X.13022)
32. Cantalapiedra JL, Prado JL, Hernández Fernández M, Alberdi MT. 2017 Decoupled ecomorphological evolution and diversification in Neogene-Quaternary horses. *Science* (*80-*.) **355**, 627–630. (doi:10.1126/science.aag1772)
33. Klingenberg CP, Marugán-Lobón J. 2013 Evolutionary covariation in geometric morphometric data: analyzing integration, modularity, and allometry in a phylogenetic context. *Syst. Biol.* **62**, 591–610. (doi:10.1093/sysbio/syt025)
34. Gould SJ, Lewontin RC. 1979 The spandrels of San Marco and the Panglossian paradigm: a critique of the adaptationist programme. *Proc. R. Soc. Lond. B* **205**, 581–598. (doi:10.1098/rspb.1979.0086)
35. Janis CM, Bernor RL. 2019 The evolution of equid monodactyly: a review including a new hypothesis. *Front. Ecol. Evol.* **7**, 1–19. (doi:10.3389/fevo.2019.00119)
36. Damuth J, Janis CM. 2011 On the relationship between hypsodonty and feeding ecology in ungulate mammals, and its utility in palaeoecology. *Biol. Rev.* **86**, 733–758. (doi:10.1111/j.1469-185X.2011.00176.x)
37. Parker AK, McHorse BK, Pierce SE. 2018 Niche modeling reveals lack of broad-scale habitat partitioning in extinct horses of North America. *Palaeogeogr. Palaeoclimatol. Palaeoecol.* **511**, 103–118. (doi:10.1016/j.palaeo.2018.07.017)
38. Maguire KC, Stigall AL. 2008 Paleobiogeography of Miocene Equinae of North America: a phylogenetic biogeographic analysis of the relative roles of climate, vicariance, and dispersal. *Palaeogeogr. Palaeoclimatol. Palaeoecol.* **267**, 175–184. (doi:10.1016/j.palaeo.2008.06.014)
39. Figueirido B, Janis CM, Pérez-Claros JA, De Renzi M, Palmqvist P. 2012 Cenozoic climate change influences mammalian evolutionary dynamics. *Proc. Natl Acad. Sci. USA* **109**, 722–727. (doi:10.1073/pnas.1110246108)
40. Hooker JJ. 2010 The 'Grande Coupure' in the Hampshire Basin, UK: taxonomy and stratigraphy of the mammals on either side of this major Paleogene faunal turnover. In *Micropalaeontology, sedimentary environments and stratigraphy: a tribute to Dennis Curry (1912–2001)* (eds JE Whittaker, MB Hart), pp. 147–215. Bath, UK: The Geological Society Publishing House. (doi:10.1144/tms004.8)
41. Blois JL, Hadly EA. 2009 Mammalian response to Cenozoic climatic change. *Annu. Rev. Earth Planet. Sci.* **37**, 181–208. (doi:10.1146/annurev.earth.031208.100055)
42. Prothero DR, Heaton TH. 1996 Faunal stability during the early Oligocene climatic crash. *Palaeogeogr. Palaeoclimatol. Palaeoecol.* **127**, 257–283. (doi:10.1016/S0031-0182(96)00099-5)
43. Blondel C. 2001 The Eocene-Oligocene ungulates from Western Europe and their environment. *Palaeogeogr. Palaeoclimatol. Palaeoecol.* **168**, 125–139. (doi:10.1016/S0031-0182(00)00252-2)
44. Prado JL, Alberdi MT. 2014 Global evolution of Equidae and Gomphotheriidae from South America. *Integr. Zool.* **9**, 434–443. (doi:10.1111/1749-4877.12064)
45. Machado H, Grillo O, Scott E, Avilla LS. 2018 Following the footsteps of the South American *Equus*: are autopodia taxonomically informative? *J. Mamm. Evol.* **25**, 397–405. (doi:10.1007/s10914-017-9389-6)
46. Prado JL, Alberdi MT. 2017 Nomenclature and taxonomy. In *Fossil horses of South America: phylogeny, systemics and ecology*, pp. 7–60. Cham, Switzerland: Springer.
47. Sondaar PY. 1977 Insularity and its effect on mammal evolution. In *Major patterns in vertebrate evolution* (eds MK Hecht, PC Goody, BM Hecht), pp. 671–707. Boston, MA: Springer US. (doi:10.1007/978-1-4684-8851-7_23)
48. Rozzi R, Varela S, Bover P, Martin JM. 2020 Causal explanations for the evolution of 'low gear' locomotion in insular ruminants. *J. Biogeogr.* **47**, 2274–2285. (doi:10.1111/jbi.13942)
49. Brown NAT, Kawcak CE, McIlwraith CW, Pandy MG. 2003 Architectural properties of distal forelimb muscles in horses, *Equus caballus*. *J. Morphol.* **258**, 106–114. (doi:10.1002/jmor.10113)
50. Soffler C, Hermanson JW. 2006 Muscular design in the equine interosseus muscle. *J. Morphol.* **267**, 696–704. (doi:10.1002/jmor.10433)
51. Hanot P, Herrel A, Guintard C, Cornette R. 2018 The impact of artificial selection on morphological integration in the appendicular skeleton of domestic horses. *J. Anat.* **232**, 657–673. (doi:10.1111/joa.12772)
52. MacLaren JA. 2021 Data from: Biogeography a key influence on distal forelimb variation in horses through the Cenozoic. Dryad Digital Repository. (https://doi.org/10.5061/dryad.x0k6djhhg)